The counterbalance of the adverse side effects of releasing agent on the properties of cementitious materials with nano-particles

Fawad Muhammad [a], Pengkun Hou [a, b, 1], Zheng Wang [c], Xiangming Zhou [b], Xin Cheng [a, 1]

[a] Shandong Provincial Key Lab for Preparation and Measurement of Building Materials, University of Jinan, Jinan, Shandong, 250022, China.

[b] Department of Civil & Environmental Engineering, Brunel University London, Uxbridge, Middlesex UB83PH, United Kingdom.

[c] Shandong Highway Group, Jinan, 250098.

Abstract: Organic releasing agent (RA) has been widely used on concrete formwork during casting and structuring for good surface quality. However, the harmful side effects introduced by the organic RA on cement hydration would finally lead to decreased property gain of hardened cementitious materials at the surface. In this work, 5*wt*% RA was added into cement paste/mortar to simulate its effects on cementitious materials at the superficial layer when applied to formwork. Moreover, nano-particles (nano-SiO_2 and nano-TiO_2) have been introduced into the RA for counterbalancing the adverse effects on cement hydration by taking advantage of cement hydration acceleration effects of nano-modification. Results showed that the incorporation of nanoparticles into RA could result in a good dispersion with ultra-sonication. The addition of 4*wt*% NS and 16*wt*% NT into RA can improve the compressive strength of mortar by 28.2% and 38.1%. Meanwhile, they decrease water absorption rate up to 41.9% and 46.2% to that of the control sample (mortar with RA). Hydration heat calorimetry results demonstrated that the reaction of RA-added cement can be accelerated by nanoparticles, resulting in the microstructure's enhanced compactness (MIP). This work shed light on the nano-modification of concrete surface in a comfortable, efficient, and economical way.

Keywords: releasing agent (RA), nano-SiO_2, nano-TiO_2, mechanical property, porosity

[1] Corresponding Authors: Pengkun Hou, mse_houpk@ujn.edu.cn, pkhou@163.com;

Xin Cheng, chengxin@ujn.edu.cn

1. Introduction

Concrete is a versatile building material used worldwide in a number of commercial and industrial infrastructures. The exterior appearance of concrete surface influences the quality of concrete for example smooth, fine surface leveling, slippage-resistant, self-cleaning surface, glossy appearance, etc. These features of concrete surface are critically important beyond their function as aggressive agents' barrier to harsh environments [1]. To ensure a high quality of surface, engineers select suitable formwork made up of metal, wood, or polymer and releasing agents (RAs are organic and inorganic) in various areas like, underground walls, floors, and balconies[2,3].

Engineers recommend high-quality releasing agents (RA's), which were pragmatic to the surface of concrete formwork. The RAs for formwork prevent sticking while presenting perfect adhesion to the formwork and reducing air bubbles get stuck on the surface during the concrete pouring [4-7].

Although RAs provide good visibility for concrete surface but create fundamental flaws for concrete [23]. Thomas et al. reported that mineral RA played a detrimental role in dropping the degree of hydration and increasing setting time due to delay the C_3A hydration and decrease total hydration rate by up to 40% [8]. The influence of oil viscosities (kerosene, crude oil, and diesel) on the high-performance concrete showed that increasing oil viscosity decreases mechanical strength [9]. Under the petroleum product's influence, the strength was reduced from 18% to 90% [10]. For the cement paste, Shao et al and Scherer et al [11, 12] similarly showed the adverse influences of petroleum products. The mechanical results of concrete demonstrated that petroleum products in hardened concrete's pores negatively affected the mechanical performances [13].

On the other hand, nanoparticles like nano-silica, nano titanium dioxides, carbon nanotube, nano alumina, C-S-H seeds, nano quartz [14-18], etc. have been introduced into cementitious materials in the past decades. Significant enhancements on the hydration reaction [19] and strengthening [20, 24] processes of cementitious materials have been well documented even when the dosage was small. The hydration seeding effect and the high pozzolanic reactivity of the nanoparticles contribute to the property gain. Moreover, multi-functionalization can be endorsed with the aid of functional nanoparticles [21, 22]. It thus could be expected that the joint-incorporation of nanoparticles with RA could counterbalance the negative side effect of RA on

cement hydration, thus improving the surface quality. Meanwhile, concrete functionalization can be easily and durably achieved at the concrete's superficial surface after formwork demolding.

In this work, nano-engineered releasing agent's (neRA's) were prepared by adding NS (2% and 4%) and NT (4% and 16%) into the releasing agent (RA), and then the mixture was added into cement to simulate the case of releasing agents meeting with cement at the superficial surface of the concrete mold. The effectiveness of nano-modification on counterbalancing the releasing agent's adverse side effects (RA) was evaluated through macro and micro-analysis to lay the foundation for the application on the surface of concrete molds, which is the other part of this project.

2. Materials and testing methods

2.1. Materials

In this study, Portland cement Type I 42.5 R, was used and its physiochemical compositions are listed in Table 1.

The mobile DTE 25 (Exxon Mobile Corporation) was used as a releasing agent (RA) and the physical properties were showed in Table 2. The Mobile oil DTE-25 selected as a RA in this work with a high viscosity 46.2 mm^2/sec at 45 □ as compare to lower viscosity release agents such as Copper State Petroleum's concrete form oil with a viscosity of 10 mm^2/sec at 40 □, THORCAST CRB with a viscosity of 7.70 mm^2/sec at 20 □ and Ortolan Extra 772 KS 10 mm^2/sec at 25 □. The advantage of Mobile Oil DTE-25 are; 1) A high viscosity of the oil enables a better dispersion and suspension of the nanoparticles. 2) A higher adhesion of the nano-modified releasing agent to the formwork can be achieved; 3) Due to the high anti-foaming property of oil, the roughness of the concrete surface has been decreased.

Nano titanium dioxide (nano-TiO_2 P.25, ~20 nm) and nano-silica (nano-SiO_2, ~7-40 nm) were purchased from MACKLIN and Aladdin China.

80 **Table 1.** Physiochemical properties of OPC I 42.5R

Material	*wt* %
Al_2O_3	4.7
CaO	62.9
Fe_2O_3	3.3
MgO	2.7
SiO_2	20.2
SO_3	3.3
LoI	1.1
Total	98.2
Surface area (m^2/kg)	380

81

82 **Table 2.** Physical properties of mobile oil DTE-25

Physical properties of Mobile oil DTE-25	
Physical state	Yellow color liquid
Odor threshold	N/D
Boiling point	316 ℃
Density	0.8667 kg/L
Flash point	238 ℃
Kinematic viscosity (45 ℃)	46.2 mm^2/s

83

84 2.2. Preparation of Nano-engineered releasing agent (neRA)

85 Two types of nanoparticles were used to modify the releasing agent (RA), nano-TiO_2 and
86 nano-SiO_2. During the preparation of neRa, nano-TiO_2 (4*wt* %, 16*wt* %) or nano-SiO_2 (2*wt* %,
87 4*wt* %) was added into the RA, and stirred for one hour at 50 °C. It was then sonicated at 40 kHz
88 for 30 minutes at 30 °C to disperse nanoparticles uniformly in RA. Four different neRA were

prepared, namely 4*wt* % TiO_2 (M5T4), 16*wt* % TiO_2 (M5T16), 2*wt* % SiO_2 (M5S2) and 4*wt* % SiO_2 (M5S4) as shown in Table 3.

Table 3. Mix proportion of nano-SiO_2, nano-TiO_2 and RA for neRA preparation

Sample ID	RA (g)	Nanoparticle (g)	Nanoparticle *wt* % of RA
RA	100 g	0	0 %
M5T4	96 g	4 g nano-TiO_2	4% nano-TiO_2
M5T16	84 g	16 g nano-TiO_2	16% nano-TiO_2
M5S2	98 g	2 g nano-SiO_2	2% nano-SiO_2
M5S4	96 g	4 g nano-SiO_2	4% nano-SiO_2

2.3. Cement based material preparation and mix design

The mix proportions of cement mortar were mixed according to the Chinese standard GB175-2007. OPC I 42.5R cement and standard sand (ratio 1/3) was prepared and mixed for two minutes. Required amount of water (w/c 0.5) was added and mixed for two minutes before adding RA/neRA. Then RA/neRA 5% added into mixture and mixed for four minutes to achieve a good mixing quality. The mortar samples for macro analysis were cast in molds with the size of (4 cm×4 cm×16 cm).

For micro analysis the cement paste samples were prepared with water to cement ratio (w/c 0.45) and cast in 50 mL tubes. All samples were cured in an ambient environment. After one day, samples were demolded and cured in a climate chamber (RH > 95%, 25 °C) until the desired test age.

2.4. Particle dispersion analysis

The particle size analyzer (American Beckman Coulter LS 13 320) was used to determine the particle size distribution of NS and NT dispersed in the RA after ultra-sonication treatment for 10-, 20-, and 30-minutes respectively.

The modified NT nano-engineered release agent (neRA) samples were dispersed in ethanol and sent to the dispenser connected to the laser diffraction instrument. The operating range of the instrument is between 0.017 and 2000 μm size of particles.

2.5. Mechanical strength

Cement mortar samples (4 cm×4 cm×16 cm) were used for compressive strength measurement according to Chines standard GBT17671-1999 [24] after 3-, 7- and 28-days of curing age.

2.6. Hydration heat measurement

The hydration heat evaluation test was performed by using an isothermal calorimeter (TAM Air) at 20 °C. Cement was first mixed with the required amount of distilled water (w/c ratio 0.45), neRA, and then the paste samples were injected into ampoules sealed by a lid and loaded into the calorimeter. The heat flow was recorded for 72 h [23].

2.7. Water absorption analysis

To measure water absorption rate of cement mortars with and without the addition of nano-engineered release agent (neRA). Cement mortar samples with a size of (4 cm×4 cm×16 cm) was cut into a size of 1 cm thick by cold saw after 7- and 28-days of curing and were kept in an oven at 50 °C for 48 hours. And then sealed four sides by resin and two sides (upper and lower) was unsealed of each sample and weighed before immersion in water [25]. The samples were then placed in a tank containing water in such a manner that the topside of the cube was lightly above the water level. After water immersion, the samples were taken out at interval of 10-minutes and after the surface water was wiped off with a wet towel, the weight was recorded. This was repeated until no significant change in weight was observed. The percentage of water absorption was calculated by using this equation

$$\text{Water absorption rate (\%)} = \frac{w2 - w1}{w1} \times 100 \quad (1)$$

w1 is the weight of sample at time 0, w2 represent the weight of sample after time t.

2.8. Mercury intrusion porosimetry

Mercury intrusion porosimetry method (AutoPore IV 9500) was used to investigate the pore size distribution in hardened mortar. The sample slices were kept in isopropanol for two days to stop hydration and then dried in a vacuum oven for 24 hours at 45 °C. Then samples were broken into small pieces. Approximately 0.7–1.0 g sample was used for each test.

2.9. Thermal-gravimetric (TG)

Thermal-gravimetric (TG) analysis was conducted using a (TG/DSC tests (Mettler Toledo, Switzerland), cement paste samples were heated from 30 °C up to 1000 °C at a rate of 10°C/min with nitrogen as a carrier gas. Before the test, samples at the age of 14-days were crushed and immersed in methanol to stop hydration for two days and then dried in the vacuum oven at 45°C for 48 hours.

3. Results and discussions

3.1. Dispersion

When mixing with other constituent materials of the concrete mixture, it is essential to confirm nano-materials' uniform dispersion. Under 10-, 20-, and 30-minutes ultrasonic treatment time for M5T4 and M5T16 neRA samples. The particle size distribution (PSD) result shows that with increasing sonication time were effected the differential volume peak (Fig.1). Fig 1a shows that with increase sonication time, the particle size distribution shifted towards lower particle sizes i.e. 1.67 µm to 1.38 µm. While sonication time 10-min, 20-min and 30-min shows 7.44 µm, 8.79 µm and 7.42 µm particles size respectively in Fig 1b. The PSA result shows, the nanoparticles were agglomerated due to the surface energy and van der Waal's attractive forces between RA molecules and NT particles [34].

The average particle size of M5T4 for sonication of 10- and 20- minutes was 1.67 µm, 1.38 µm, respectively. The M5T16 sample average size was 7.44 µm, 8.79 µm for 10- and 20-minutes sonication while for 30-minutes sonication, the M5T4 and M5T16 sample shows multi-peak: first peak at 1.66 µm, 1.52 µm and second peak at 7.42 µm, 8.14 µm, respectively.

The multi peaks were observed in 30-minutes sonication in Fig.1 (a and b). The bimodal peak shows the presence of two different size of nano-particles dispersion which may lead to become

agglomerated with increasing sonication [25]. With increasing sonication time up to 10- and 20-minutes, the particles size became smaller size (Fig.1) [26].

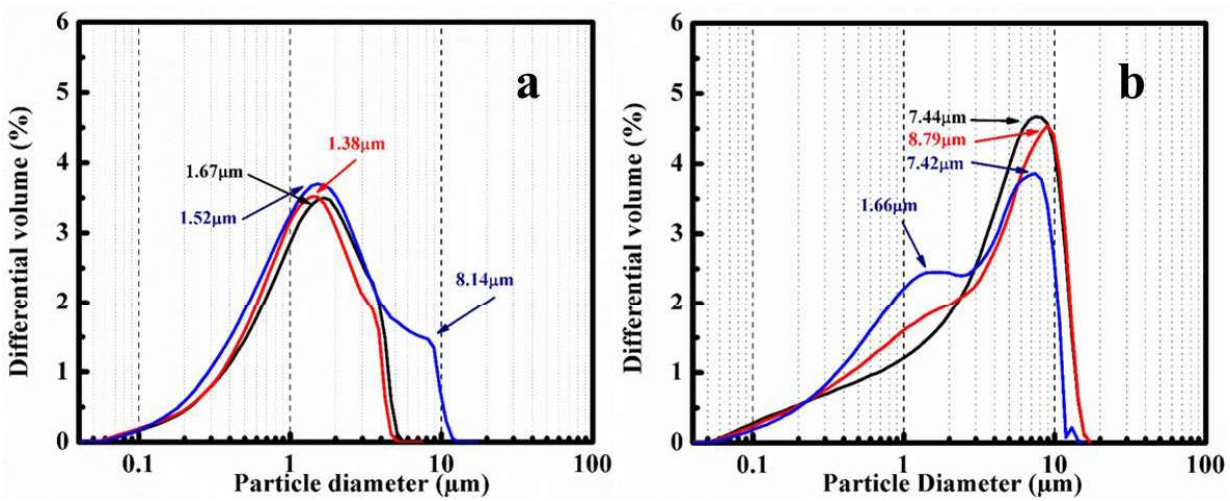

Fig. 1. Dispersion of nano-TiO_2 in RA by different ultra-sonication time (a) M5T4, (b) M5T16

3.2. Compressive strength

To assess the influences of release agent (RA) and nano engineered release agent (neRa) on the compressive strength property of cement-based materials, the compressive strength of cement mortar with the addition of RA and neRa at different ages (3-,7-, 14- and 28-days) were evaluated, and the results are shown in Fig.2.

It shows that the increase in the compression resistance of all cement mortar specimens increases as the curing age expected. Also, cement mortar specimens with neRa additive showed greater compressive strength than the sample of the RA compared to blank sample.

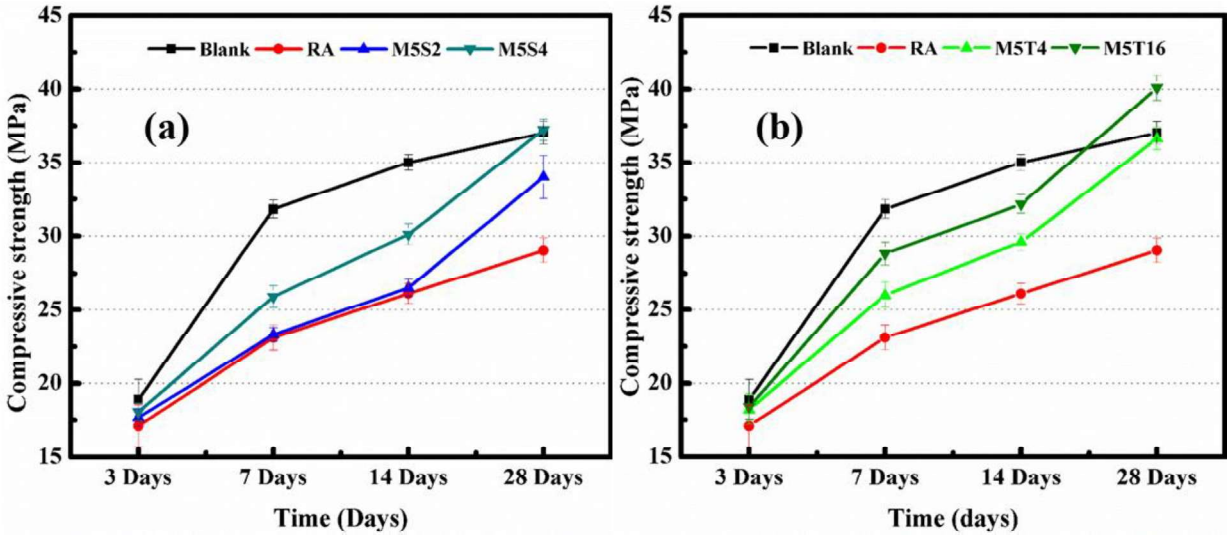

Fig. 2. Compressive strength after 3-, 7-, 14- and 28-days of curing age of (a) NS (nERa) (b) NT (nERa) cement mortar samples

RA, M5S2 reduced their strength by 27.4% and 26.7% at 7 days of curing age and this could be due to very low dosage of nano-particles and indicated the effect of RA on cement hydration at early ages. While M5T4, M5T16 and M5S4 also decreased by 18.3%, 9%, and 18%, respectively compared to control sample (without RA). The effect of RA on cement mortar strength was greatly influence at early curing age due decrease degree of hydration which was proved by cement hydration results.

The strength enhancement effect of neRa on cement mortar was more noticeably shown in Table 4 at 28-day compressive strength (%) compared with the control sample (without RA). The compressive strength of M5S4 and M5T16 cement mortar sample increased by 8.29% and 0.6%.

While the compressive strength of the RA, M5S2 and M5T4 cement mortar samples decreased by 21.6%, 8.12% and 1.08%. Compared with the early age strength, it shows that neRa contributes greater to later age compressive strength.

189 **Table 4.** Compressive strength (%) as compared to blank cement mortar sample

Curing age	RA	M5T4	M5T16	M5S2	M5S4
7 Days	-27.4	-18.3	-9.46	-26.8	-18.7
28 Days	-21.6	-1.08	8.29	-8.12	0.57

190

191 3.3. Cement hydration

192 The influence of RA and neRA as an admixture on the mechanical strength has been
193 mentioned. The isothermal calorimetric results are shown in Fig.3 for the blank, RA, and neRa
194 samples. Fig.3a and Fig.3b shows that the addition of RA, decreased hydration rate of the
195 cement. However, after a period of 30 hours, the effect of M5S2 and M5T4 were also decreased
196 the rate of hydration. While the addition of M5S4 and M5T16 increase the rate of hydration.
197 Meanwhile, retardation was observed in hydration heat peak with RA and neRA modified
198 cement. The retardation of the exothermic peak increased with RA, M5S2, and M5T4 content.
199 While decrease with the addition of M5S4 and M5T16 shown in Fig.4a and 4b.
200 The ending point of the induction period of RA was delayed due to the presence of oil which
201 effect the C_3A hydration, while hydration of C_3A retardation decreased with the addition of neRA
202 shown in Fig.4. The induction period of RA sample was delayed up to (6.3h), which were more
203 than M5S2 (2.3h), M5S4 (4.9h), M5T4 (2.32h), M5T16 (4.7h).
204 After the induction period, the cement hydration enters an accelerated period, and the
205 nucleation of hydrates grows rapidly. The hydration rate of the acceleration period was
206 determined by the total number of C-S-H hydrate nuclei.
207 The addition of RA greatly impacted on C_3S hydration has seen by the delay of the
208 acceleration period up to 19.3h and also lower heat of hydration, while the addition of M5S2 and
209 M5T4 caused a peak delay up to 13.3h and 14h respectively due to counterbalancing effect of NS
210 and NT. As the dosage of nanoparticles in neRa increases, the heat intensity of M5S4 and M5T16
211 increases, shortening by 8.4h and 8.35h, respectively.

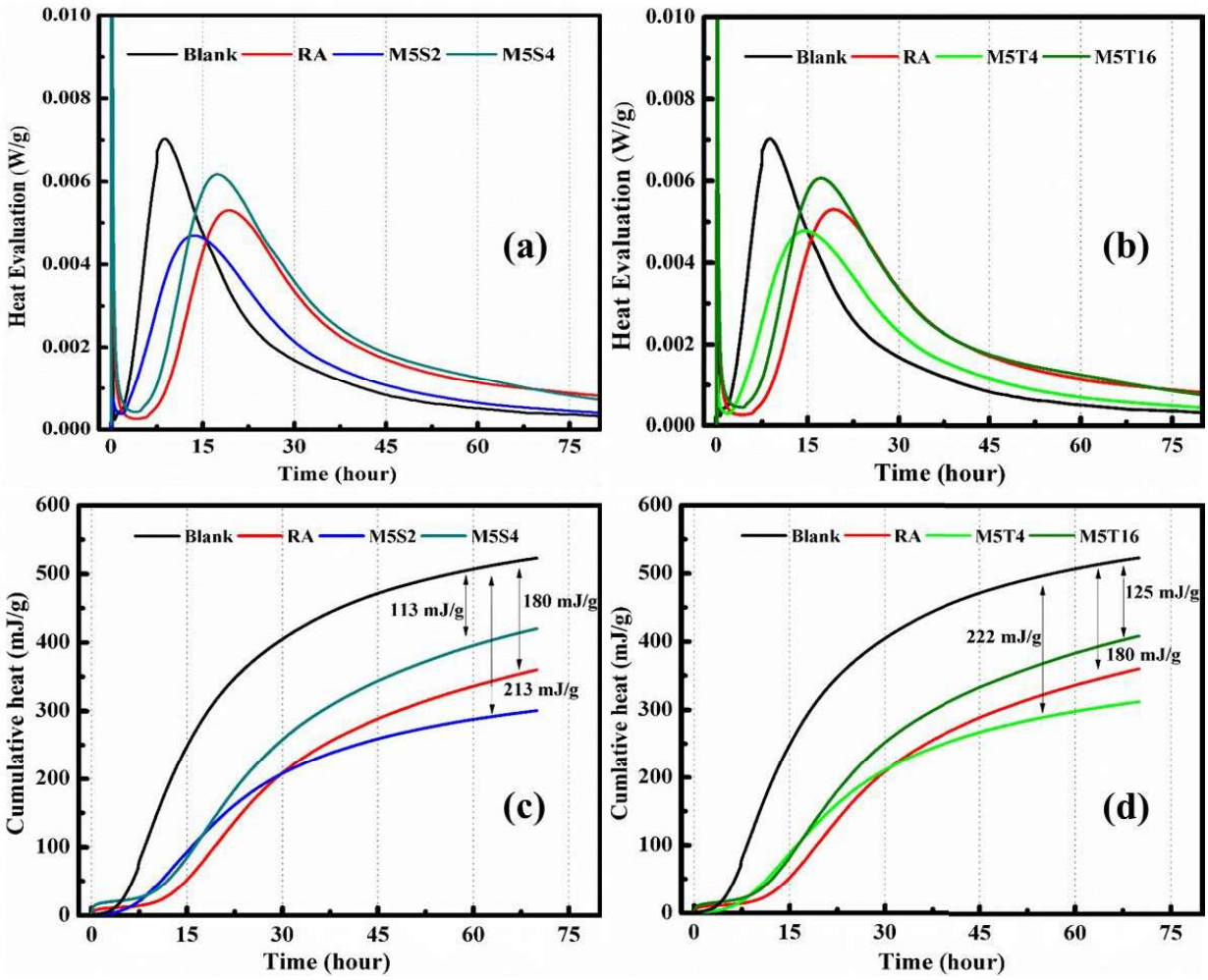

Fig. 3. Thermal calorimetry results of (a,c) NS (nERa) samples (b,d) NT (nERa) samples

Therefore in Fig.4, nanoparticles do not seem to lead to higher final hydration, but they improve hydration dynamics when compared to RA. This observation is due to 1) the pozzolanic activity of NS [29, 30], and 2) the seeding effect provided by NT for the formation of hydration products which finally increase the hydration rate as compared to RA.

NS and NT with a specific ratio had same cumulative heat of hydration in the all measurement periods, indicating unequivocally that the accelerated hydration compensated for the effect of their releasing agent in cement paste even at early stage of hydration [31-33].

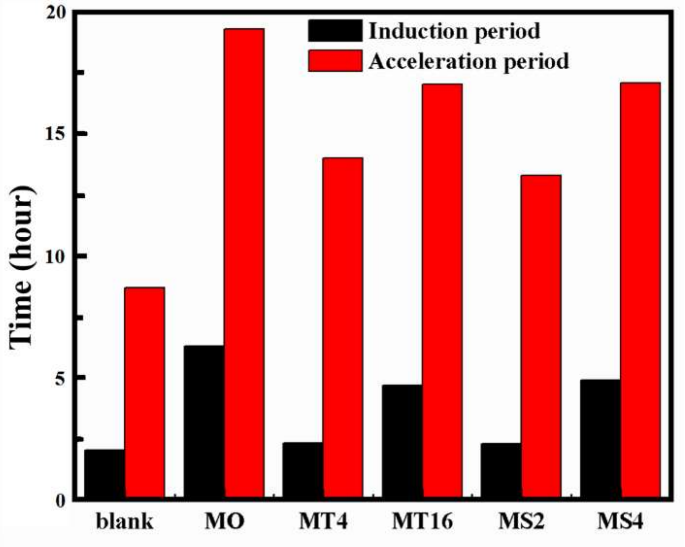

Fig. 4. Time difference of induction phase and acceleration phase

3.4. Water absorption rate

The influences of RA and neRA on the water absorption rate of mortar samples results shown in Fig.5. After 7-days of curing, Fig.5 shows that the water absorption rate of neRA samples was increased steadily. As mentioned in Table.5 the early age neRA samples had a higher water absorption rate than RA sample. The water absorption rates of M5T4 and M5T16 at 6h was 5.3% and 5.2%, while M5S2 and M5S4 increased by 5.1% and 5.7%, respectively. The early water absorption rate of RA sample was 3.98% lower than neRA samples.

Table 5. Water absorption rate (%) of RA, MS and MT mortar sample after 7- and 28-days curing age

Curing Age	Blank	RA	M5T4	M5T16	M5S2	M5S4
7 Days	5.51%	3.98%	5.3%	5.2%	5.1%	5.7%
28 Days	4.6%	4.7%	4.3%	2.57%	3.5%	2.77%

Later age, after 28-days curing water absorption rate of M5T4 and M5T16 was 4.3% and 2.57%. M5S2 and M5S4 water absorption rate was 3.5% and 2.77%, while blank and RA samples water absorption rate was 4.6% and 4.7%, respectively. The water absorption rate of neRA

modified cement mortars was remarkably decreased at later ages as shown in Fig.5 (c and d). The decreased water absorption rate of neRA samples after 28 days curing age is thought to be related to the fact that NS and NT increased chemically bound water due to the higher hydration rate [27]. While the MIP results showed the evidenced that increase the dosage of NS and NT decrease the threshold pore diameter and this phenomenon directs significant properties for cement durability.

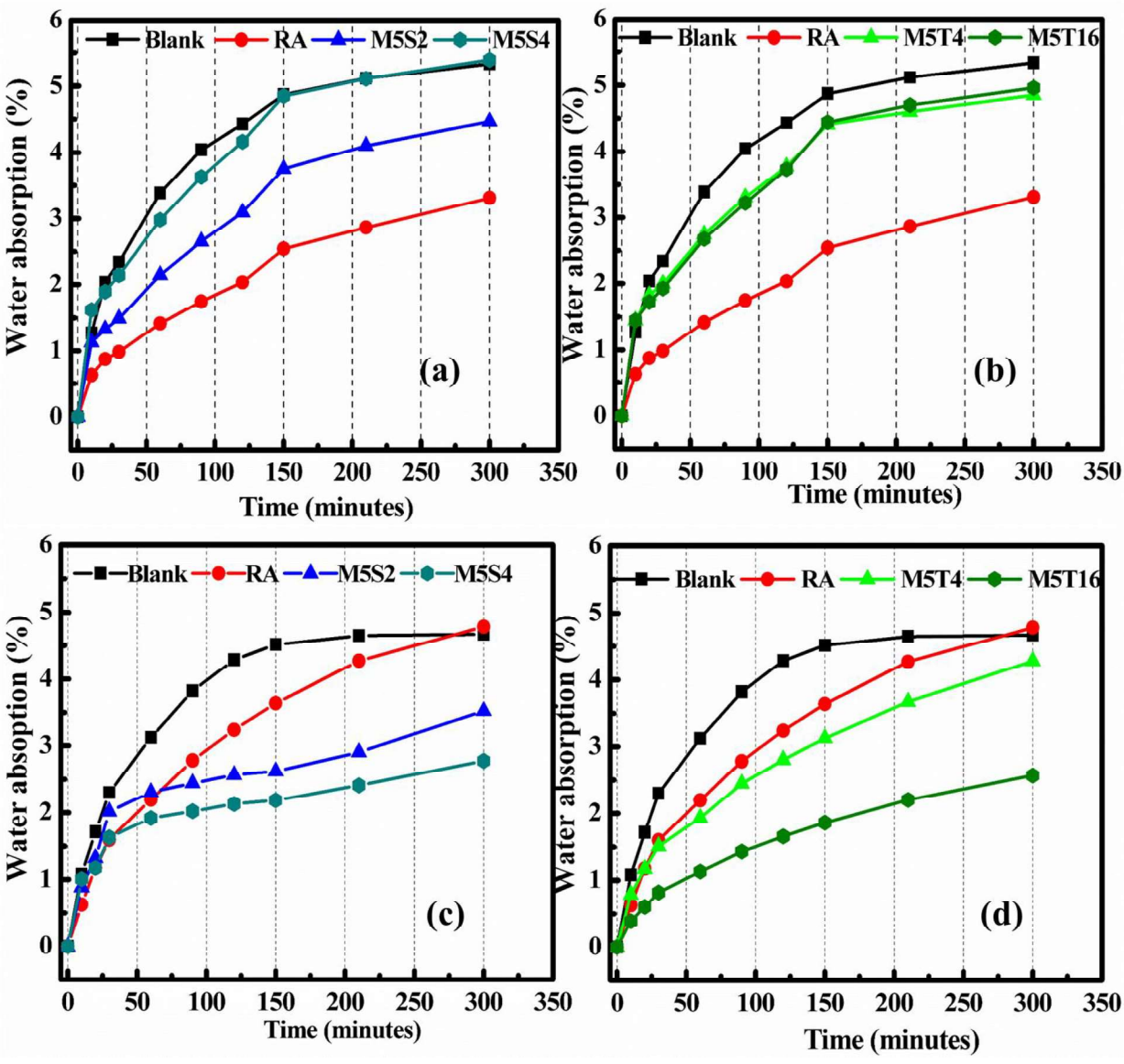

Fig. 5. Water absorption rate % (a) NS sample after 7-days (b) NT sample after 7-days, (c) NS sample after 28-days (d) NT sample after 28-days

3.5. Mercury intrusion porosity

246 The first intrusion was observed for sealed cured pastes at a pore entry diameter of around 0.1
247 μm. This corresponds to the threshold pore diameter. After that, two main intrusion steps can be
248 observed at 1 μm and in the range 0.01-0.1 μm.
249 Pore size distribution and porosity of cement paste were shows below in Fig.6. The
250 noticeable difference of the porosity after adding different percentages of M5T4, M5T16, M5S2,
251 and M5S4 ensured the good comparability of the porosity with the samples macro properties of
252 the reference RA sample. While increasing the concentration of NS and NT in neRA a significant
253 reduction of threshold pore diameter.
254 The addition of NS in RA, can decrease the number of larger pores and also reduce the
255 detrimental pores size which convert to harmless pores which size below 0.1 μm due to the
256 pozzolanic activity of NS [28]. In Fig.6 (d) shows that NT decrease the size of pores in the range
257 of 0.1-1 μm and significantly decrease the number of pores. The reason may be attributed to the
258 addition of nanoparticles filling the larger pores size and refining the sample's microstructure.
259 The total porosity of RA sample was 13.18% which is higher than the M5S2, M5S4, M5T4
260 and M5T16. The total porosity of NS and NT added RA samples were 11.44%, 8.2%, %, 11.04%
261 and 7.1% which show that compressive strength was not only effected by hydration product but
262 also effected by total porosity reduction.

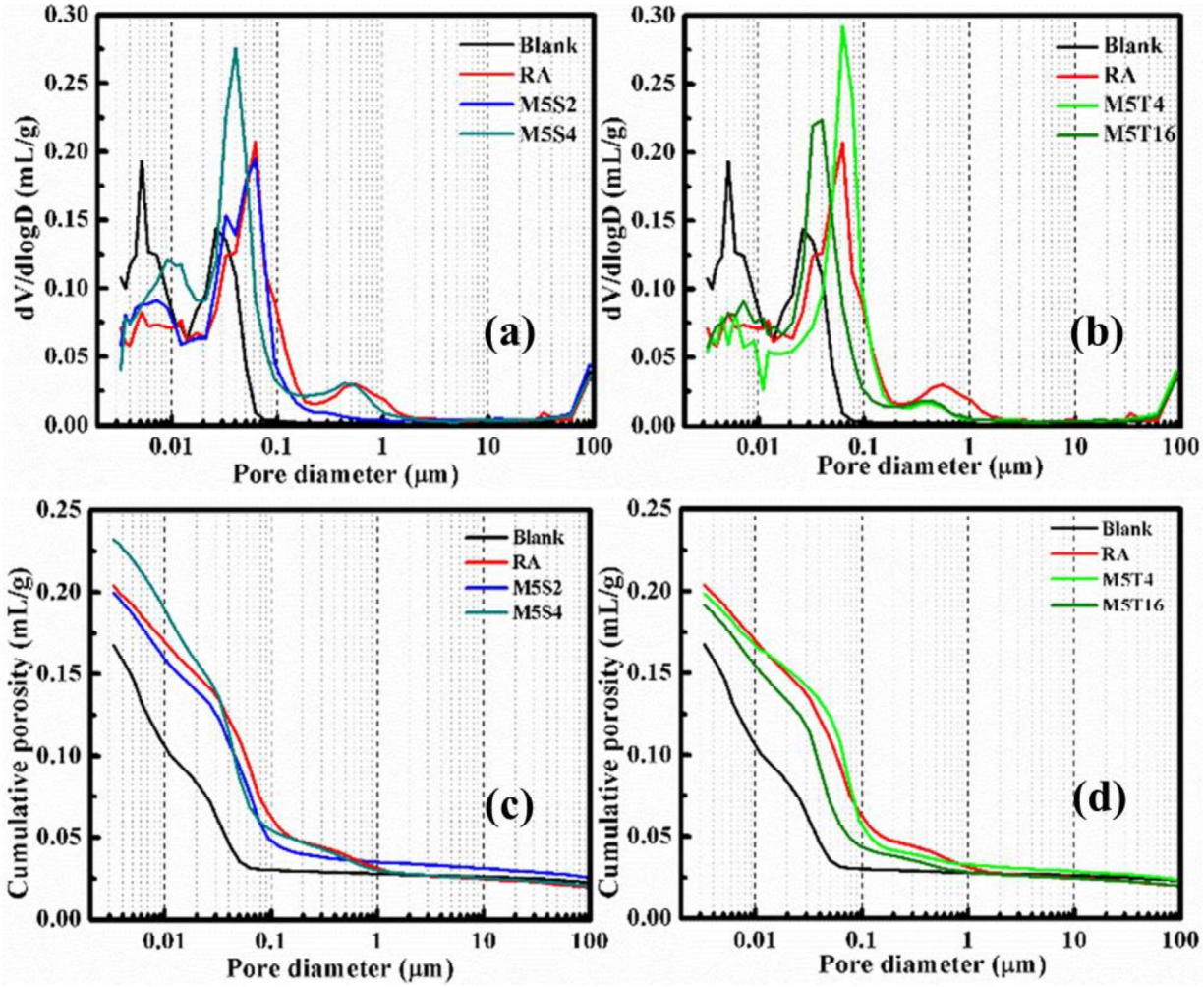

Fig. 6. Mercury intrusion porosimetry curves for NS (a, c) and NT (b, d) cement paste samples

3.6. TG/DTG analysis

In order to quantitatively study the content of ettringite, portlandite (CH), and calcite ($CaCO_3$) in this work, TG analysis was carried out according to work Kim's. In this process, the decomposition temperature ranges of 30-1000 °C was used for quantitative extraction of the content.

The weight losses in the interval of 30–200 ℃ were mainly associated with the decomposition process of water, CSH, and AFt. The weight losses in the 400–500 ℃ and 600–800 ℃ were attributing to the decomposition of CH and decarbonation of $CaCO_3$, respectively. The total number of CH can be calculated by the following equation:

$$\mathrm{CH}\ (\%) = \mathrm{Mass1} \times \frac{74}{18} + \mathrm{Mass2} \times \frac{74}{44} \quad (2)$$

Where Mass1 is the reduction of mass caused by dehydration of CH and Mass2 is the mass loss due to the decomposition of Calcite respectively; and molecular weight of water, CO_2 and CH 18, 44 and 74, respectively.

The decomposition was calculated by using two different methods 1: tangent method and 2: step vise method, calculate all the ettringite, CH, and calcite decomposition with temperature. Table 6 shows the mean value of calculated mass reduction due to the decomposition of ettringite, CH and calcite.

Table 6. Mass (%) reduction with respect to temperature

Sample	**30-200** ℃	**400-600** ℃	**600-800** ℃
Blank	8.49	26.33	3.43
Oil	7.72	24.16	5.99
MT4	8.52	22.61	2.32
MT16	9.16	20.65	3.71
MS2	8.74	23.94	3.05
MS4	9.08	22.56	3.93

It was observed that the formation of ettringite 7.72 % which is relatively smaller in the RA sample than neRA samples. Fig.7 shows that for neRA added samples increase the formation of ettringite, decline the content of CH, and calcite could be due to the limited CH consuming capacity, therefore a large number of C-S-H formed, with contribution to the improvement of strength and porosity. While RA sample high CH and calcite content; which were higher weight loss than all neRA and blank samples.

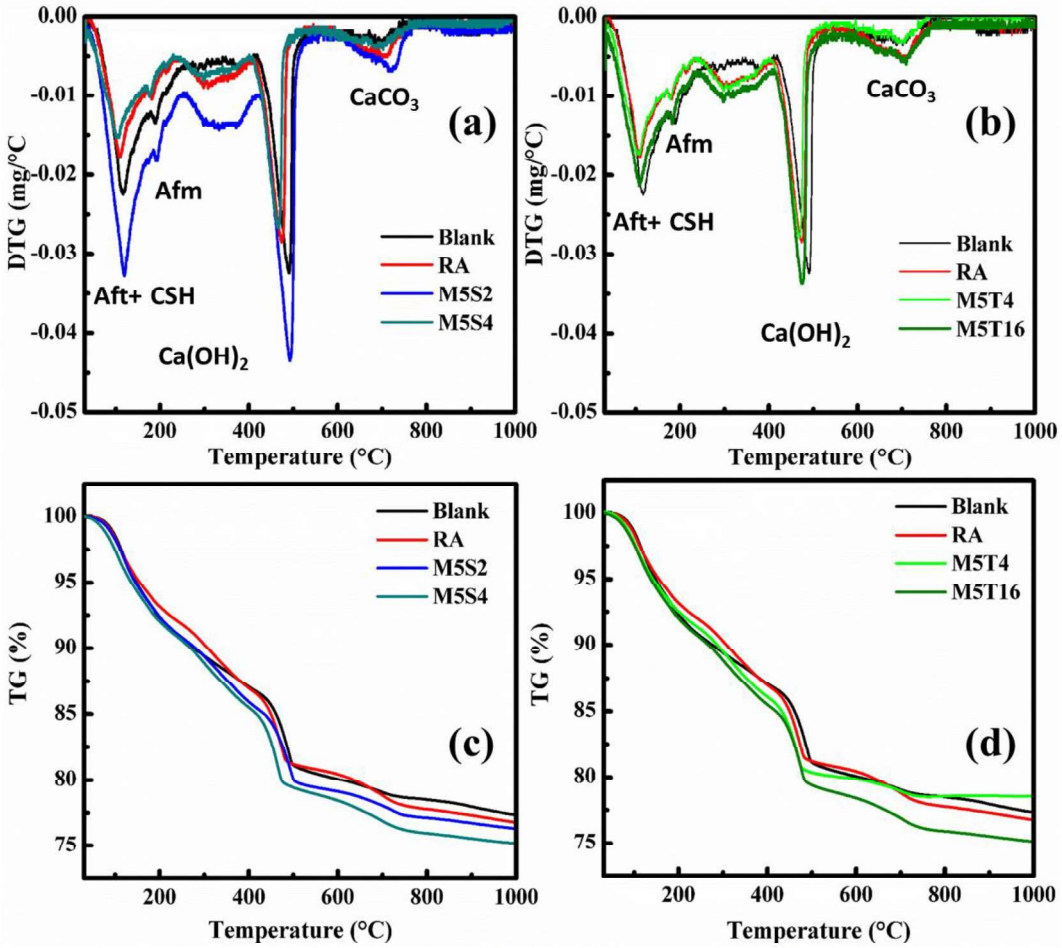

Fig. 7. DTG/TG % curve of samples (a, c) for MS sample & (b, d) for MT samples

4. Conclusions

In this study, the RA/neRA influence in cement mortar/paste was investigated through a variety of methods. From the above results and discussions the following conclusions can be drawn

1. NS 4*wt* % and NT 16*wt* % added into RA can considerably increase the compressive strength by 28.2 %, 38.1 % comparable to RA sample.
2. Samples with the addition of neRA (NS 4*wt* % and NT 16*wt* %) can significantly increase the rate of hydration due to the pozzolanic activity and formation of nuclei compared to RA sample.
3. Water absorption rate significantly declines in neRA (NS 4*wt* % and NT 16*wt* %) added samples by 41.9 % and 46.2 % compared to RA added sample due to compactness of

303 microstructure which lead to the decrease of total porosity (NS 4*wt* % and NT16*wt* %) by
304 8.2 % and 7.1 % as compared to RA sample.
305 The summary of this study demonstrated that the addition of nano-SiO_2 or nano-TiO_2 into
306 RA counterbalanced the negative effects of the latter to cement hydration on concrete surface,
307 which further sheds light on the advantages of further multi-functionalization of concrete surface
308 through this effective and economical nano-engineering.

309 ## Acknowledgment

310 The authors gratefully acknowledge supports from Shandong Natural Science Foundation
311 (ZR2020YQ33), Education Department of Shandong Province (2019GGX102077), Science and
312 Technology Innovation Support Plan for Young Researchers in Institutes of Higher Education in
313 Shandong (2019KJA017), Case-by-Case Project for Top Outstanding Talents of Jinan, and the
314 Taishan Scholars Program (ts201712048). This project has also received funding from the
315 European Union's Horizon 2020 research and innovation program under the Marie Skłodowska-
316 Curie grant agreement No [893469].

317 ## Reference

318 [1] Chi, J.; Zhang, G.; Xie, Q.; Ma, C.; Zhang, G., High performance epoxy coating with
319 cross-linkable solvent via Diels-Alder reaction for anti-corrosion of concrete. Prog. Org.
320 Coat. 139 (2020) 105473.
321 [2] Holmes, N.; Dunne, K.; O'Donnell, J., Longitudinal shear resistance of composite slabs
322 containing crumb rubber in concrete toppings, Construct. Build. Mater. 55 (2014**)** 365-
323 378.
324 [3] Hurd, M., High-performance plywoods For concrete forming. Concr. Constr 1997, 202.
325 [4] Libessart, L.; de Caro, P.; Djelal, C.; Dubois, I., Correlation between adhesion energy of
326 release agents on the formwork and demoulding performances. Construct. Build. Mater.
327 76 (2015) 130-139.
328 [5] Coniglio, N.; Spitz, N.; El Mansori, M., Designing metallic surfaces in contact with
329 hardening fresh concrete: A review. Construct. Build. Mater. 255 (2020) 119384.

[6] Assaad, J. J., Disposing used engine oils in concrete – Optimum dosage and compatibility with water reducers. Construct. Build. Mater. 44 (2013) 734-742.

[7] Libessart, L.; Djelal, C.; de Caro, P.; Laiymani, I., Comparative study of the tribological behaviour of emulsions and demoulding oils at the concrete/formwork interface. Construct. Build. Mater. 239 (2020) 117826.

[8] Almabrok, M. H.; McLaughlan, R.; Vessalas, K.; Thomas, P, Effect of oil contaminated aggregates on cement hydration. Am.J.Eng.Res.(2019) 81-89.

[9] Jasim, A. T.; Jawad, F. A., Affect of oil on strength of normal and high performanc concrete. Al-Qadisiyah Journal for Engineering Sciences. 3 (1) (2010) 24-32.

[10] Ajagbe, W. O.; Omokehinde, O. S.; Alade, G. A.; Agbede, O. A., Effect of crude oil impacted sand on compressive strength of concrete. Construct. Build. Mater. 26 (1) (2012) 9-12.

[11] Yurtdas, I.; Xie, S. Y.; Burlion, N.; Shao, J. F.; Saint-Marc, J.; Garnier, A., Influence of chemical degradation on mechanical behavior of a petroleum cement paste. Cement. Concrete. Res. 41 (4) (2011) 412-421.

[12] Zhang, J.; Weissinger, E. A.; Peethamparan, S.; Scherer, G. W., Early hydration and setting of oil well cement. Cement. Concrete. Res. 40 (7) (2010) 1023-1033.

[13] Kameche, Z. A.; Ghomari, F.; Choinska, M.; Khelidj, A., Assessment of liquid water and gas permeabilities of partially saturated ordinary concrete. Construct. Build. Mater. 65 (2014) 551-565.

[14] Thomas, J. J.; Jennings, H. M.; Chen, J. J., Influence of nucleation seeding on the hydration mechanisms of tricalcium silicate and cement. J. Phys. Chem. C. 113 (11) (2009) 4327-4334.

[15] Lavergne, F.; Belhadi, R.; Carriat, J.; Ben Fraj, A., Effect of nano-silica particles on the hydration, the rheology and the strength development of a blended cement paste. Cem. Concr. Compos. 95 (2019) 42-55.

[16] Jayapalan, A.; Lee, B.; Kurtis, K., Effect of nano-sized titanium dioxide on early age hydration of Portland cement. In Nanotechnology in construction 3, Springer (2009) 267-273.

[17] Land, G.; Stephan, D., Controlling cement hydration with nanoparticles. Cem. Concr. Compos. 57 (2015) 64-67.

[18] Chen, J.; Kou, S.-c.; Poon, C.-s., Hydration and properties of nano-TiO_2 blended cement composites. Cem. Concr. Compos. 34 (5) (2012) 642-649.

[19] Xu, S.; Xie, N.; Cheng, X.; Huang, S.; Feng, L.; Hou, P.; Zhu, Y., Environmental resistance of cement concrete modified with low dosage nano particles. Construct. Build. Mater. 164 (2018) 535-553.

[20] Guo, Z.; Wang, Y.; Hou, P.; Shao, Y.; Zuo, X.; Li, Q.; Xie, N.; Cheng, X., Comparison study on the sulfate attack resistivity of cement-based materials modified with nanoSiO_2 and conventional SCMs: Mechanical strength and volume stability. Construct. Build. Mater. 211 (2019) 556-570.

[21] Wang, D.; Yang, P.; Hou, P.; Zhang, L.; Zhang, X.; Zhou, Z.; Xie, N.; Huang, S.; Cheng, X., Cement-based composites endowed with novel functions through controlling interface microstructure from Fe_3O_4@SiO_2 nanoparticles. Cem. Concr. Compos. 80 (2017) 268-276.

[22] Wang, D.; Hou, P.; Zhang, L.; Yang, P.; Cheng, X., Photocatalytic and hydrophobic activity of cement-based materials from benzyl-terminated-TiO_2 spheres with core-shell structures. Construct. Build. Mater. 148 (2017) 176-183.

[23] C. Djelal, P. de Caro, I. Dubois, L. Libessart, N. Pebere, Comprehension of demoulding mechanisms at the formwork / oil / concrete interface. Materials & Structures, 41 (2008) 571-581.

[24] Nazari, A.; Riahi, S.; Riahi, S.; Shamekhi, S. F.; Khademno, A., Influence of Al_2O_3 nanoparticles on the compressive strength and workability of blended concrete. Am. J. Sci. 6 (5) (2010) 6-9.

[25] Joni, I. M.; Purwanto, A.; Iskandar, F.; Okuyama, K., Dispersion stability enhancement of titania nanoparticles in organic solvent using a bead mill process. Ind. Eng. Chem. Res.48 (15) (2009) 6916-6922.

[26] Fernandes, C. N.; Ferreira, R. L.; Bernardo, R. D.; Avelino, F.; Bertini, A. A., Using TiO_2 nanoparticles as a SO_2 catalyst in cement mortars. Construct. Build. Mater. 257 (2020) 119542

[27] Kushimoto, K.; Ishihara, S.; Pinches, S.; Sesso, M. L.; Usher, S. P.; Franks, G. V.; Kano, J., Development of a method for determining the maximum van der Waals force to

391 analyze dispersion and aggregation of particles in a suspension. Adv. Powder. Technol. 31
392 (6) (2020) 2267-2275.
393 [28] Wang, J.; Du, P.; Zhou, Z.; Xu, D.; Xie, N.; Cheng, X., Effect of nano-silica on hydration,
394 microstructure of alkali-activated slag. Construct. Build. Mater. 220 (2019) 110-118.
395 [29] Chen R, Zhang Z, A Comparative study on the pozzolanic activity between nano-SiO_2 and
396 silica fume. J. Wuhan Univ. Technol. Mater. Sci. Ed. 21 (2006) 153–157.
397 [30] Shuai Bai, Xinchun Guan, Guoyu Li; Effect of the early-age frost damage and nano-SiO_2
398 modification on the properties of Portland cement paste. Construct. Build. Mater. 262
399 (2020) 120098.
400 [31] JinbangWang, XinCheng, ZonghuiZhou; Optimizing the content of nano-SiO_2, nano-TiO_2
401 and nano-$CaCO_3$ in Portland cement paste by response surface methodology.
402 J. Build. Eng. 35 (2021) 102073
403 [32] Yeonung J, Sung-H, Min O. Acceleration of cement hydration from supplementary
404 cementitious materials: Performance comparison between silica fume and hydrophobic
405 silica. Cem. Concr. Compos. 112 (2020) 103688
406 [33] Jun C, Shi K, Chi-S. Hydration and properties of nano-TiO_2 blended cement composites.
407 Cem. Concr. Compos. 34 (2012) 642-649.
408 [34] R. Maheswaran a , J. Sunil. Effect of nano sized garnet particles dispersion on the viscous
409 behavior of extreme pressure lubricant oil. J. Mol. Liq. 223 (2016) 643-651.
410
411